BIOCHEMISTRY
including biophysical chemistry & molecular biology
Article

Biochemistry **2010,** *49,* 6083–6092 6083
DOI: 10.1021/bi1000454

Specificity and Membrane Partitioning of Grsp1 Signaling Complexes with Grp1 Family Arf Exchange Factors†

Jonathan P. DiNitto,‡ Meng-Tse Lee, Andrew W. Malaby, and David G. Lambright*

Program in Molecular Medicine and Department of Biochemistry and Molecular Pharmacology, University of Massachusetts Medical School, Worcester, Massachusetts 01605. ‡Present address: Biogen Idec, Hemophilia Therapeutic Area, 9 Fourth Ave., Waltham, Massachusetts 02451.

Received January 12, 2010; Revised Manuscript Received June 6, 2010

ABSTRACT: The Arf exchange factor Grp1 selectively binds phosphatidylinositol 3,4,5-triphosphate [PtdIns-(3,4,5)P_3], which is required for recruitment to the plasma membrane in stimulated cells. The mechanisms for phosphoinositide recognition by the PH domain, catalysis of nucleotide exchange by the Sec7 domain, and autoinhibition by elements proximal to the PH domain are well-characterized. The N-terminal heptad repeats in Grp1 have also been shown to mediate homodimerization in vitro as well as heteromeric interactions with heptad repeats in the FERM domain-containing protein Grsp1 both in vitro and in cells [Klarlund, J. K., et al. (2001) *J. Biol. Chem. 276*, 40065−40070]. Here, we have characterized the oligomeric state of Grsp1 and Grp1 family proteins (Grp1, ARNO, and Cytohesin-1) as well as the oligomeric state, stoichiometry, and specificity of Grsp1 complexes with Grp1, ARNO, and Cytohesin-1. At low micromolar concentrations, Grp1 and ARNO are homodimeric whereas Cytohesin-1 and Grsp1 are monomeric. When mixed with Grsp1, Grp1 homodimers and Cytohesin-1 monomers spontaneously re-equilibrate to form heterodimers, whereas approximately 50% of ARNO remains homodimeric under the same conditions. Fluorescence resonance energy transfer experiments suggest that the Grsp1 heterodimers with Grp1 and Cytohesin-1 adopt a largely antiparallel orientation. Finally, formation of Grsp1−Grp1 heterodimers does not substantially influence the binding of Grp1 to the headgroups of PtdIns(3,4,5)P_3 or PtdIns(4,5)P_2, nor does it influence partitioning with liposomes containing PtdIns(3,4,5)P_3, PtdIns(4,5)P_2, and/or phosphatidylserine.

Stimulation of cells with agonists such as insulin and EGF results in activation of phosphatidylinositol 3-kinase (PI-3 kinase) (*2*−*4*), leading to transient accumulation of the lipid second messenger phosphatidylinositol (PtdIns)[1] 3,4,5-trisphosphate [PtdIns(3,4,5)P_3]. Production of PtdIns(3,4,5)P_3 controls diverse cellular processes through plasma membrane recruitment of proteins and protein complexes, including Grp1. Grp1 (also termed Cytohesin-3) belongs to the homologous Grp1 family of functionally related Arf guanine nucleotide exchange factors (GEFs) that includes ARNO (Cytohesin-2) and Cytohesin-1. Grp1, ARNO, and Cytohesin-1 have a modular architecture consisting of N-terminal heptad repeats, a Sec7 domain with exchange activity for Arf1 and Arf6, a pleckstrin homology (PH) domain, and a C-terminal polybasic sequence (*5*). The Grp1 PH domain selectively binds PtdIns(3,4,5)P_3 with high affinity and is essential for plasma membrane targeting (*6*, *7*). Localization of Grp1 family proteins to the plasma membrane and subsequent activation of Arfs have been implicated in a variety of cellular processes, including adhesion, endocytic trafficking, cell motility, T-cell anergy, helper T-cell activation, and insulin signaling (*8*).

EST and Affymetrix gene chip transcriptomes indicate that ARNO and Cytohesin-1 are ubiquitously expressed whereas Grp1 is broadly expressed, though at relatively low levels in certain tissues such as liver, thymus, and peripheral blood lymphocytes (*9*, *10*). Grsp1 was originally isolated from a mouse brain cDNA expression library probed with Grp1 and shown by Western blotting to be expressed at significant levels in brain and lung, where Grp1 is also highly expressed (*1*). A subsequent analysis by RT-PCR suggests that Grsp1 is expressed at high levels in other tissues as well, including kidney, spleen, heart, and bone marrow (*11*). Grsp1−Grp1 complexes were readily detected by coprecipitation in lysates from cotransfected COS-1 cells, but not in mixed lysates from separately transfected cells, and complexes of the endogenous proteins have been coprecipitated from mouse lung homogenates (*1*). Grsp1 contains several putative protein−protein interaction domains, including an N-terminal FERM domain, which is followed by two heptad repeat regions with a high propensity to form coiled coils (*12*). Deletion mapping indicated that the interaction between Grp1 and Grsp1 is mediated by the N-terminal heptad repeats in Grp1

†This work was supported by National Institutes of Health Grant DK060564.

*To whom correspondence should be addressed: Program in Molecular Medicine, Two Biotech, 373 Plantation St., Worcester, MA 01605. Telephone: (508) 856-6876. Fax: (508) 856-4289. E-mail: David.Lambright@umassmed.edu.

[1]Abbreviations: Grp1, general receptor for phosphoinositides; Grsp1, Grp1 signaling partner; Arf, ADP ribosylation factor; ARNO, Arf nucleotide binding site opener; CASP, Cytohesin-1-associated scaffold protein; GRASP, Grp1-associated scaffold protein; FERM, band 4.1, ezrin, radixin, moesin; Ins, inositol; PtdIns, phosphatidylinositol; PtdSer, phosphatidylserine; PtdCho, phosphatidylcholine; SUV, small unilamelar vesicle; IPTG, isopropyl β-D-galactopyranoside; NiNTA, nickel nitrilotriacetic acid; 6xHis, hexahistidine; GST, glutathione *S*-transferase; SDS−PAGE, sodium dodecyl sulfate−polyacrylamide gel electrophoresis; Tris, tris(hydroxymethyl)aminomethane; FRET, fluorescence resonance energy transfer; FE, FRET efficiency; LE, labeling efficiency; ITC, isothermal titration microcalorimetry; co-IP, co-immunoprecipitation.

Published on Web 06/07/2010

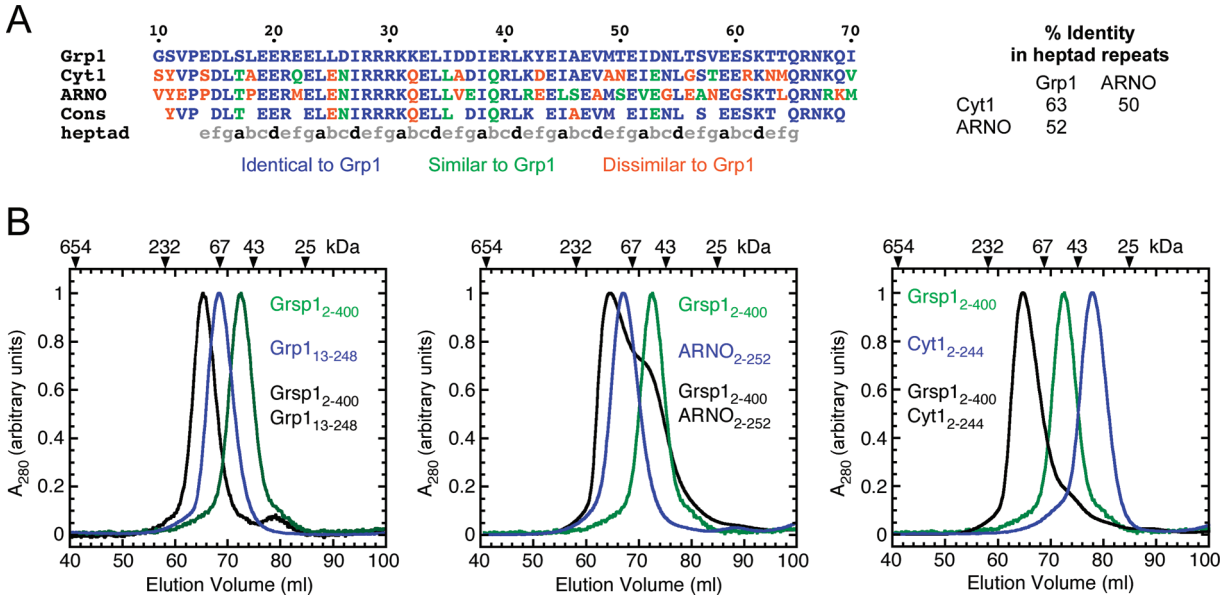

FIGURE 1: Isolation of Grsp1 complexes by gel filtration on Superdex-200. (A) Comparison of the amino acid sequences of Grp1, ARNO, and Cytohesin-1 within the heptad repeat region. (B) Proteins at 15 μM were incubated overnight at 4 °C and injected onto a Superdex-200 column. Elution volumes for globular molecular mass standards are indicated above each chromatogram.

and the first of the two heptad repeat regions in Grsp1 (*1*). FERM domains have been shown to mediate high-affinity protein−protein interactions with the cytoplasmic domains of integral membrane proteins, including CD44 and ICAM-2 (*13*). The multiple protein−protein interaction motifs present in Grsp1 suggest that it may function as a molecular scaffold. The Grsp1−Grp1 complex colocalizes with cortical actin rich regions in response to stimulation of CHO-T cells with insulin or EGF (*1*). Taken together, these data suggest Grp1 may function not only to activate Arf proteins at the cell membrane but also to recruit additional functionality to the cell membrane in response to extracellular signals.

The presence of a phosphoinositide specific PH domain in Grp1 and a putative protein or lipid binding FERM domain in Grsp1 is consistent with the possibility that both protein−lipid and protein−protein interactions may contribute to localization and/or assembly into higher-order complexes. In mouse lung tissue extracts, a Grsp1 antibody coprecipitated only a small amount of the total Grp1 whereas a Grp1 antibody coprecipitated Grsp1 almost quantitatively (*1*). This suggests that a substantial portion of Grp1 would be available to interact with other proteins. Indeed, Grp1 has been shown to interact with several other proteins, including CASP (Cytohesin-1-associated scaffold protein) and GRASP (Grp1-associated scaffold protein) (*14*, *15*). The epitope for interaction with these proteins has been mapped to the heptad repeats of Grp1. Among Grp1, ARNO, and Cytohesin-1, this region shows the greatest sequence diversity [50−63% identical (Figure 1A)]. The higher degree of sequence variability within the heptad repeats raises the possibility that the individual members of the Grp1 family may be capable of assembling into functionally distinct complexes.

To gain further insight into the intrinsic properties of Grsp1 complexes, we have characterized the stability, specificity, and oligomeric state of Grsp1 complexes with Grp1, Cytohesin-1, and ARNO. The results demonstrate that Grsp1 readily forms heterodimers with both Grp1 and Cytohesin-1. Whereas Grp1 heterodimers form at the expense of less stable Grp1 homodimers, ARNO homodimers are at least as stable as Grsp1−ARNO heterodimers. FRET experiments suggest that Grsp1−Grp1 and Grsp1−Cytohesin-1 heterodimers preferentially assemble in an antiparallel orientation. Formation of the Grsp1−Grp1 complex, however, does not enhance partitioning with membranes containing PtdIns(3,4,5)P_3 or PtdIns(4,5)P_2.

EXPERIMENTAL PROCEDURES

Constructs, Expression, and Purification. Constructs of mouse Grp1 ("2G" diglycine splice variant, GenBank entry AF001871), human ARNO ("3G" triglycine splice variant, GenBank entry X99753), human Cytohesin-1 ("3G" triglycine splice variant, GenBank entry BC050452), and mouse Grsp1 (GenBank entry AF327857) were amplified using Vent DNA polymerase (New England Biolabs). For Grp1 and ARNO, the human and mouse proteins are identical within the heptad repeats. Human and mouse Cytohesin-1 differ by only two substitutions, both of which are conservative in nature and are not located in the a or d position of the heptad repeat. The first heptad repeat regions of human and mouse Grsp1 are 94% identical with one substitution at the first d position and two substitutions at other (non-a or -d) positions. Amplified constructs were inserted into a modified pET15b vector (Novagen) containing an N-terminal 6xHis tag (MGHHHHHHGS) using *Bam*HI and *Sal*I restriction sites. The GST−Grsp1$_{350-400}$ construct used for coprecipitation assays was inserted into the *Bam*HI and *Sal*I restriction sites of pGEX-6P1 (Amersham Pharmacia Biotech). For FRET experiments, a cysteine residue was added to either the N- or C-terminus of each protein. Constructs were verified by sequencing the coding region from both 5′ and 3′ directions.

Constructs were expressed in BL21(DE3)RIL cells (Stratagene) grown in 2× YT-amp (16 g of bacto tryptone, 10 g of bacto yeast extract, 5 g of NaCl, and 100 mg of ampicillin per liter). Cultures were grown to an OD_{600} of 0.4 and induced with isopropyl 1-thio-β-D-galactopyranoside for 16 h at 20 °C. For the purification of 6xHis proteins, cells were suspended in lysis buffer [50 mM Tris-HCl (pH 8.0), 0.1% β-mercaptoethanol, 0.1 mM phenylmethanesulfonyl fluoride, 1 mg/mL lysozyme, 2 mM $MgCl_2$, and 10 μg/mL DNase I] and disrupted by sonication. Triton X-100 was then

added to a final concentration of 0.5%, and the cell lysate was centrifuged at 35000*g* for 45 min. The supernatant was loaded on a Ni-NTA column (Qiagen) equilibrated with buffer [50 mM Tris-HCl (pH 8.0) and 0.1% β-mercaptoethanol], washed with 20 column volumes of buffer containing 15 mM imidazole, and eluted with a gradient from 10 to 150 mM imidazole. Subsequent ion exchange chromatography on a Source-S or Source-Q column (GE Healthcare) followed by gel filtration chromatography over Superdex-200 (GE Healthcare) yielded protein preparations that were >99% pure as judged by SDS−PAGE. For the GST−Grsp1$_{350-400}$ construct, the clarified supernatant was mixed with glutathione-Sepharose (GE Healthcare) equilibrated with buffer [50 mM Tris-HCl (pH 8.0), 150 mM NaCl, and 0.1% β-mercaptoethanol] and nutated at 4 °C for 30 min. The resin was centrifuged at 500*g* and washed with three times with 20 mL of buffer. The GST fusion protein was eluted with buffer containing 10 mM glutathione. The GST−Grsp1$_{350-400}$ fusion protein was >99% pure as judged by SDS−PAGE.

Formation of the Grsp1−Grp1 Complex and Gel Filtration Chromatography. A 2 mL solution of 30 μM Grp1$_{13-248}$ was mixed with an equal volume of 30 μM Grsp1$_{2-400}$ in buffer [50 mM Tris-HCl (pH 8.0), 150 mM NaCl, 10% glycerol, and 0.1% β-mercaptoethanol] and incubated at 4 °C for 16 h. The sample was then filtered through a 0.2 μm acrodisc and loaded on a Superdex-200 column (GE Healthcare). Equal amounts of the free proteins were loaded on a Superdex-200 column under identical conditions to allow direct comparison of the elution profiles. Fractions were analyzed via 15% SDS−PAGE with Coomassie blue staining. The Superdex-200 column was calibrated using a gel filtration calibration kit (GE Healthcare) with ribonuclease A (13.7 kDa), chymotrypsinogen A (25 kDa), ovalbumin (43 kDa), albumin (67 kDa), aldolase (158 kDa), catalase (232 kDa), ferritin (440 kDa), and thyroglobulin (654 kDa) as molecular mass standards.

Coprecipitation. The GST−Grsp1$_{350-400}$ fusion protein at a concentration of 21 μM was incubated with an equivalent molar quantity of either 6xHis Grp1$_{13-399}$, 6xHis ARNO$_{2-400}$, or 6xHis Cytohesin-1$_{2-398}$ in buffer [50 mM Tris-HCl (pH 8.0), 150 mM NaCl, and 0.1% β-mercaptoethanol] at 4 °C for 2 h on a nutator. Glutathione-sepharose beads were added to the protein mixture and nutated for 1 h at 4 °C. After centrifugation at 500*g*, the supernatant was collected, the pellet was washed three times with 100 μL of buffer, and the beads were nutated for 1 h at 4 °C in buffer containing 10 mM glutathione. The supernatants and bead elutions were analyzed by 15% SDS−PAGE with Coomassie blue staining. Controls with GST substituted for the GST−Grsp1$_{350-400}$ fusion protein were also conducted to determine the amount of nonspecific binding. The gel was scanned and the integrated intensity of each band on the gel determined using NIH Image (http://rsb.info.nih.gov/nih-image).

Co-Immunoprecipitation. Full-length Grp1, Cytohesin-1, and ARNO in pEGFP-c1 and the HA-tagged brain isoform of Grsp1 in pCMV5 were generated as described previously (*1*, *16*). COS-1 cells on 15 cm dishes were cotransfected using Fugene-6 (Roche) according to the manufacturer's instructions. The cells were lysed 48 h after transfection in ice-cold lysis buffer [50 mM Tris-HCl (pH 7.5), 150 mM NaCl, 1 mM EDTA, 25 mM sodium fluoride, 1 mM sodium orthovanadate, 1% Nonidet P-40, and 1 mM dithioerythritol] supplemented with complete EDTA-free Protease Inhibitor Cocktail Tablets (Roche). One milligram of protein lysate was incubated with 50 μL of HA antibody Agarose Immobilized conjugate (Bethyl Laboratories, S190−107) overnight at 4 °C on a nutator. Immunoprecipitates captured by the HA−agarose conjugate were washed in lysis buffer four times and resuspended in 2× SDS−PAGE gel loading buffer. A rabbit anti-GFP antibody (Abcam, ab6556) and HRP-conjugated goat anti-rabbit IgG (Promega, W4011) were used for immunoblotting with chemiluminescence-based detection.

Sedimentation Equilibrium. 6xHis-tagged constructs of individual proteins and 1:1 complexes were dialyzed overnight against buffer [10 mM Tris-HCl (pH 8.0) and 200 mM NaCl] and centrifuged to equilibrium at 20 °C in an Optima XL1 analytical ultracentrifuge (Beckman Instruments). Sedimentation analysis was conducted at various protein concentrations. The absorbance at 280 nm was measured as a function of radial distance (r) from the axis of rotation using the dialysis buffer as a blank. The abscissa was transformed as $\sigma_m(r_0^2 - r^2)/2$, where r_0 was taken as the data point farthest from the axis of rotation and σ_m was calculated with SEDINTERP (*17*) using the monomer molecular mass for each construct. Data were fit to the function

$$A_{280}(r) = C_0 + \sum_i C_i \exp[-n_i\sigma_m(r_0^2 - r^2)/2]$$

where C_0 and C_i are constants and n_i represents the order of the ith oligomeric species. In the case of the Grsp1 complexes, σ_m was calculated using the molecular mass for the heterodimeric complex.

Labeling of Peptides with Alexa Fluor Dyes. 6xHis-tagged proteins corresponding to the heptad repeat region of Grp1, ARNO, Cytohesin-1, and Grsp1 were purified as described above. A single cysteine was added at either the amino-terminal (MGHHHHHHGSC-peptide) or carboxyl-terminal (MGHHHHHHGS-peptide-C) end to facilitate selective labeling of either terminus. Prior to labeling, peptide samples were exhaustively dialyzed against 50 mM sodium borate (pH 7.5) and 100 mM NaCl for 24−36 h to remove 2-mercaptoethanol present in the storage buffer. The single cysteine in each peptide was labeled with Alexa Fluor-546 (donor) or Alexa Fluor-647 (acceptor) by dilution of a stock protein solution to 100−150 μM in buffer [50 mM sodium borate (pH 7.5 or 7.0) and 100 mM NaCl]. Potential disulfide bonds were reduced by addition of a 10-fold molar excess of TCEP [tris(2-carboxyethyl)phosphine (Pierce Scientific)] to the samples. The stock Alexa Fluor dye solution in dimethyl sulfoxide was diluted to 10 mM and added to the reduced peptide solution to give a 1.1-fold molar excess of the dye. The reaction was conducted at 25 °C for 2 h or at 4 °C overnight. During labeling steps, samples were protected from light. Labeling was terminated by addition of β-mercaptoethanol to a final concentration of 0.1%. Free dye was separated from labeled peptide using a D-salt gel filtration column (Pierce Scientific) followed by exhaustive dialysis against 50 mM sodium borate (pH 7.5 or 7.0). The labeling efficiency was determined by comparison of the absorbance at the λ_{max} of the dye and the amount of peptide present determined by amino acid analysis. Labeling efficiencies of 85% for Grsp1-N and 50% for Grp1 and Cytohesin-1 peptides were obtained.

Fluorescence Resonance Energy Transfer (FRET) Experiments. FRET measurements were taken using a Tecan Safire microplate spectrometer and Corning half-area 96-well microplates. Alexa Fluor-labeled peptides were mixed in 1:1 stoichiometric amounts (2.5 μM each) in buffer [10 mM Tris (pH 8.0) and 100 mM NaCl]. The optimal excitation wavelength was determined to minimize direct excitation of the acceptor

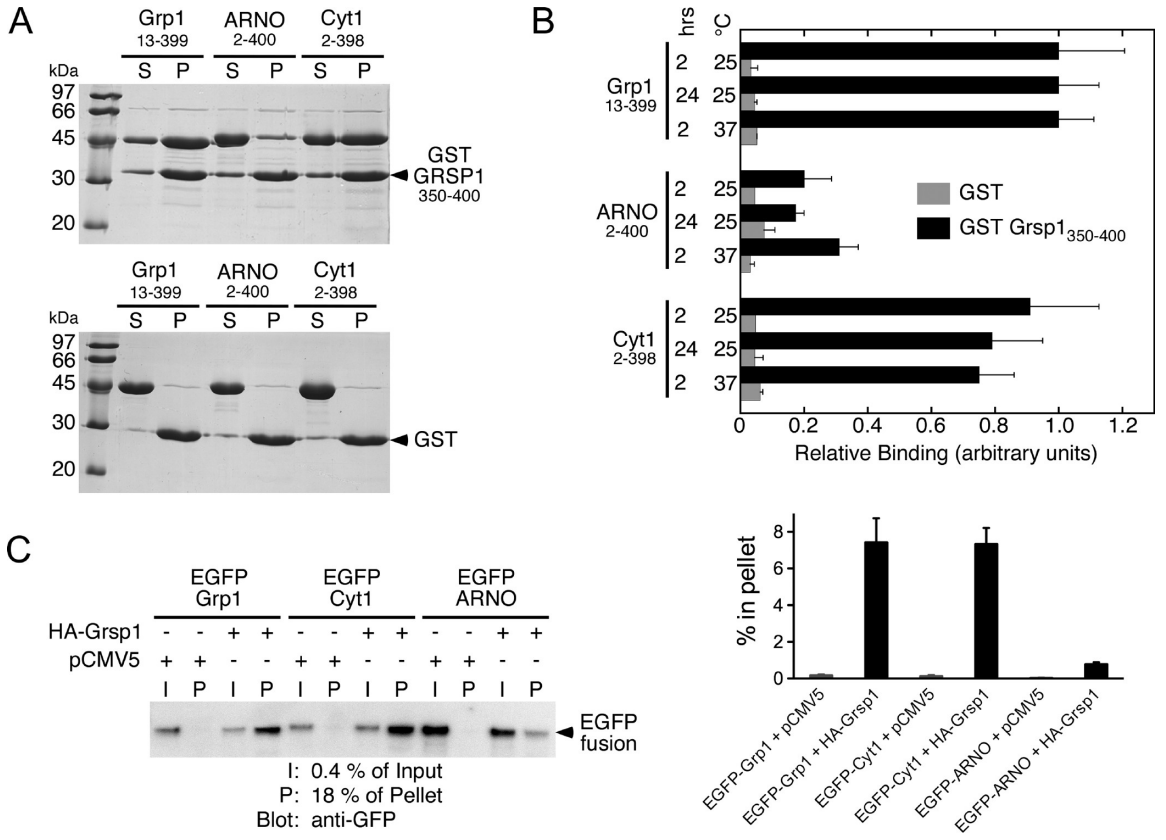

FIGURE 2: Coprecipitation and co-immunoprecipitation of Grp1, ARNO, and Cytohesin-1 with Grsp1. (A) Coprecipitation using 15 μM 6xHis $Grp1_{13-399}$, 6xHis $ARNO_{2-400}$, or 6xHis $Cytohesin_{2-398}$ with 15 μM GST−$Grsp1_{350-400}$ (top) or GST alone (bottom). (B) Quantification of coprecipitation experiments with incubation times and temperatures as indicated. The relative amount of 6xHis protein coprecipitated with the GST−$Grsp1_{350-400}$ construct or GST alone was determined by scanning the gel and quantifying individual bands using ImageJ. Integrated intensities were corrected for background. Bars and error bars represent the mean ± standard deviation for three or four independent experiments (GST fusions) or mean ± difference from the mean for two independent experiments (GST controls). (C) Co-immunoprecipitation of full-length EGFP−Grp1, EGFP−Cytohesin-1, or EGFP−ARNO constructs with full-length HA-Grsp1 48 h after cotransfection of COS-1 cells. The percentage in the pellet was determined from the integrated intensities after background correction using GelEval. Bars and error bars represent the mean ± standard error of the mean for three independent experiments.

Alexa-647 while maximizing the donor emission. Bandwidths of 5.0 nm were used for both the excitation and emission monochromators to minimize the donor fluorescence bleed-through into the acceptor channel. The emission spectra of the donor, in the presence and absence of the acceptor, were used to calculate the observed FRET efficiency (FE_{obs}) as $(I_d - I_{da})/I_d$, where I_{da} is the donor emission intensity of the sample containing both the donor and the acceptor and I_d is the emission intensity of the donor alone. Assuming the labeled and unlabeled peptides bind with equal affinity, the observed FRET efficiency was corrected for the labeling efficiency by

$$FE_{corr} = FE_{obs}/(LE_d \times LE_a)$$

where LE_d and LE_a are the labeling efficiencies for the donor and acceptor, respectively. Predicted distances were determined using the EEA1 coiled-coil structure as a model [Protein Data Bank (PDB) entry 1joc]. The uncertainty in the predicted distances was estimated by measuring the distance from the cysteine linker to the center of the fluorophore in an extended conformation.

Liposome Partitioning. Small unilamellar vesicles (SUVs) were prepared by mixing lipid stocks in chloroform in the appropriate molar ratios followed by drying to form a lipid film. To facilitate efficient sedimentation of liposomes, 1,2-distearoyl-(dibromo)-*sn*-glycero-3-phosphocholine was used. Lipids resuspended in assay buffer [50 mM Tris (pH 8.0), 200 mM KCl, and 1 mM $MgCl_2$] were frozen in liquid nitrogen and thawed for 10 cycles followed by bath sonication for 30 min and extrusion through polycarbonate membranes with a 100 nm pore size. Partitioning assays were conducted with 2 μM protein or protein complex and varying amounts of total lipid. Reaction mixtures were incubated at 25 °C for 1 h followed by centrifugation at 100000*g* for 1 h at 25 °C. Vesicle pellets were suspended in SDS sample buffer in a volume equal to that of the supernatant. Samples were analyzed via SDS−PAGE, and the amount of bound and free proteins was determined using GelEval. Each band was enclosed with a rectangle and the intensity of all the pixels in the rectangle integrated after background subtraction. The background was determined by averaging the pixel intensity above and below the band of interest. The percent pelleted was calculated as the integrated intensity of the pellet divided by the sum of the integrated intensity in the supernatant and pellet.

RESULTS

At protein concentrations in the low micromolar range, Grp1 and ARNO form stable homodimers whereas Cytohesin-1 is predominately monomeric (*16*, *18*, *19*). Homodimerization requires the heptad repeats, which also mediate heteromeric interactions with other proteins. In the case of Grp1, heteromeric complexes with Grsp1 have been detected in vitro and in cells (*1*).

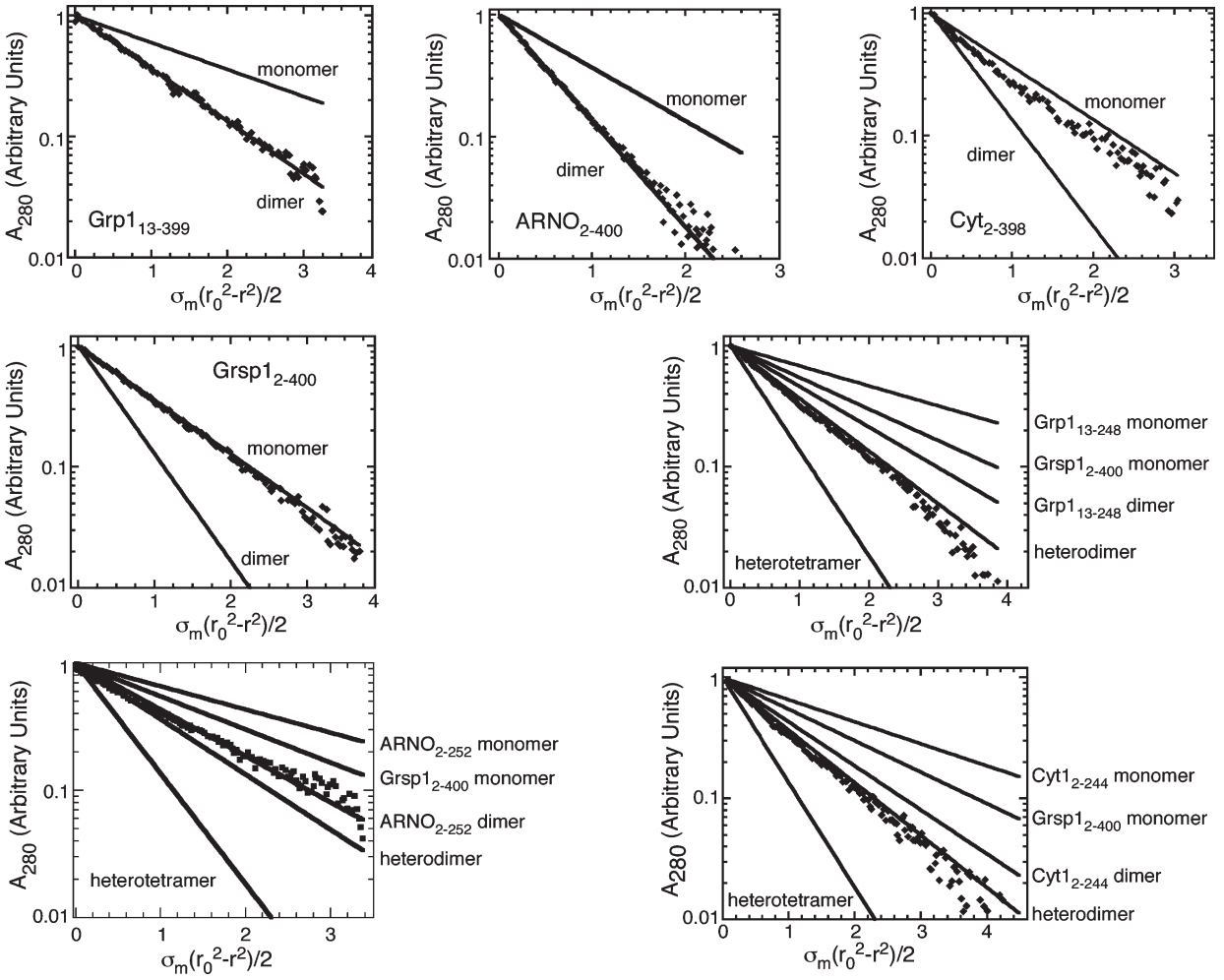

FIGURE 3: Sedimentation equilibrium experiments for Grp1 and Grsp1 constructs and Grsp1 complexes with Grp1, ARNO, and Cytohesin-1. Solid lines represent predicted model functions based on the calculated molecular mass for each species.

The region of Grsp1 that binds to Grp1 has been mapped to the first of two heptad repeat regions C-terminal to the FERM domain and has a strong propensity to form a coiled-coil structure (*12*) as do the heptad repeats in Grp1, ARNO, and Cytohesin-1. However, the stability of the heteromeric complexes compared with those of Grp1 homodimers is poorly characterized as is the specificity for Grp1 family proteins.

As one approach to determine the specificity of Grsp1 for the Grp1 family, a 6xHis Grsp1 construct spanning the N-terminal FERM domain and first heptad repeat region ($Grsp1_{2-400}$) was incubated with an equivalent molar quantity of a 6xHis Grp1, ARNO, or Cytohesin-1 construct consisting of the heptad repeats and Sec7 domain (hr-Sec7). After incubation for 16 h at 4 °C, the protein mixtures were analyzed by gel filtration chromatography (Figure 1; see also Figure 4 for calculated molecular masses). The hr-Sec7 construct was used for these experiments to allow homodimers to be clearly distinguished from heterodimers. In the absence of other proteins, $Grsp1_{2-400}$ and Cytohesin-1 elute as a monomeric species whereas Grp1 and ARNO have elution volumes larger than that expected for a globular homodimer but smaller than that expected for a globular homotrimer, consistent with an elongated homodimeric species. After incubation, Grp1 and $Grsp1_{2-400}$ coelute as a single peak with an elution volume smaller than that of either protein alone and in the expected range for a heterodimer. A similar elution profile is observed after incubation of $Grsp1_{2-400}$ and Cytohesin-1. The small tails in the elution profiles likely represent residual free species and could be due to incomplete formation of heteromeric complexes. In the case of the ARNO construct, on the other hand, two overlapping peaks are observed. The first peak contains both $Grsp1_{2-400}$ and ARNO and has an elution volume corresponding to that of the apparent heterodimeric species observed for the Grp1 and Cytohesin-1 complexes. The second peak contains predominately $Grsp1_{2-400}$ and has an estimated elution volume similar to that of the free monomer. Using Gaussian functions to model the individual peaks in the elution profiles and calculated extinction coefficients, it was estimated that approximately 50% of the $Grsp1_{2-400}$ is bound to ARNO whereas more than 90% is bound to Grp1 and Cytohesin-1.

As an alternative method for analyzing the specificity of Grsp1 for Grp1 family proteins, a Grsp1 construct containing the first heptad repeat region ($Grsp1_{350-400}$) fused to GST was used to coprecipitate Grp1, ARNO, or Cytohesin-1 constructs containing the heptad repeats and Sec7 domain. Stoichiometric amounts of either Grp1, ARNO, or Cytohesin-1 were mixed with the GST−$Grsp1_{350-400}$ construct and incubated overnight at 4 °C. At a concentration of 21 μM, the majority of Grp1 and at least 50% of Cytohesin-1 coprecipitate with the GST−$Grsp1_{350-400}$ construct whereas the majority of ARNO remains in the supernatant (Figure 2A). The extent of coprecipitation in all three cases is not significantly altered by incubation for 2 or 24 h at

	MW (kDa)		
	calculated	experimental	n_{obs}
$Grp1_{13-399}$	46.3	93.5 ± 2.7	2.02 ± 0.06
$Grp1_{13-248}$	28.5	57.9 ± 4.8	2.03 ± 0.17
$Grp1_{63-399}$	40.3	42.4 ± 1.6	1.05 ± 0.04
$ARNO_{2-400}$	47.5	94.0 ± 0.9	1.98 ± 0.02
$ARNO_{2-252}$	29.3	56.0 ± 3.5	1.91 ± 0.12
$ARNO_{60-400}$	40.8	48.4 ± 3.6	1.09 ± 0.09
$Cyt\text{-}1_{2-398}$	47.3	61.0 ± 6.6	1.29 ± 0.13
$Cyt\text{-}1_{2-244}$	29.5	49.3 ± 13.2	1.67 ± 0.45
$Cyt\text{-}1_{53-398}$	41.5	46.0 ± 2.4	1.11 ± 0.06
$Grsp1_{2-400}$	47.4	44.5 ± 1.4	0.93 ± 0.03
$Grsp1_{2-309}$	37.2	34.6 ± 0.7	0.92 ± 0.02
$Grsp1_{2-400}$ + $Grp1_{13-248}$	75.9	69.8 ± 1.5	0.92 ± 0.02
$Grsp1_{2-400}$ + $ARNO_{2-252}$	76.7	58.3 ± 5.4	0.76 ± 0.07
$Grsp1_{2-400}$ + $Cyt\text{-}1_{2-244}$	76.9	83.8 ± 2.5	1.09 ± 0.03

FIGURE 4: Comparison of observed and calculated molecular masses from sedimentation equilibrium experiments. Observed molecular masses represent the mean ± standard deviation or deviation from the mean for two to six determinations.

25 °C or 2 h at 37 °C, suggesting the binding reactions have reached equilibrium within the 2 h incubation period (Figure 2B). Thus, the relative amounts of the Grsp1 complex formed are unlikely to be due to a kinetic effect limited by the dissociation rate of the homodimers.

As a third approach, the full-length HA-tagged brain isoform of Grsp1 (HA-Grsp1) was used to co-immunoprecipitate EGFP fusions of Grp1, Cytohesin-1, or ARNO following cotransfection of COS-1 cells. As shown in Figure 2C, the EGFP fusions of all three proteins were detected in immunoprecipitates with HA-Grsp1. However, the amount of the EGFP−ARNO fusion protein in the immunoprecipates was consistently less than that of the EGFP−Grp1 and EGFP−Cytohesin-1 fusion proteins, even though the EGFP−ARNO protein appeared to express at a higher level. Taken together, the gel filtration, coprecipitation, and co-immunoprecipitation experiments indicate that (i) Grsp1−Grp1 heterodimers are considerably more stable than Grp1 homodimers, (ii) Cytohesin-1 can form stable heterodimers with Grsp1, and (iii) ARNO homodimers are at least as stable if not moderately more stable than Grsp1−ARNO heterodimers.

The oligomeric state of the individual proteins and heteromeric complexes was further analyzed by sedimentation equilibrium experiments in the concentration range from 9 to 18 μM. In an earlier study, we noted that the catalytic activity of Grp1, ARNO, and Cytohesin-1 constructs as well as a Grsp1−Grp1 complex does not correlate with a qualitative assessment of the oligomeric state consistent with sedimentation equilibrium experiments (*16*). Here, we present the data for the sedimentation equilibrium experiments along with quantitative analyses of the oligomeric state and comparisons with the calculated models for monomeric, dimeric, and heterodimeric species. We also extend the experiments and analyses to include Grsp1 alone and in combination with ARNO and Cytohesin-1. At concentrations similar to those used in the gel filtration and coprecipitation experiments, constructs of Grp1 and ARNO that include the heptad repeats are uniformly dimeric whereas the analogous Cytohesin-1 constructs have an equilibrium distribution consistent with a mixture of monomers and dimers (Figures 3 and 4 and Figure S1 of the Supporting Information). $Grsp1_{2-400}$, which includes the FERM domain and first heptad repeat region, is uniformly monomeric as is a shorter construct corresponding to the FERM domain alone. The $Grsp1_{2-400}$ complexes with $Grp1_{13-248}$ and $Cytohesin\text{-}1_{2-244}$ spanning the heptad repeats and Sec7 domain are centrifuged with a nearly uniform size distribution close to the predicted model for an ideal heterodimeric species and clearly distinguishable from $Grsp1_{2-400}$ and $Cytohesin\text{-}1_{2-244}$ monomers as well as $Grp1_{13-248}$ dimers (Figures 3 and 4). Conversely, the solution containing $Grsp1_{2-400}$ and the $ARNO_{2-252}$ construct has a size distribution in the range expected for $ARNO_{2-252}$

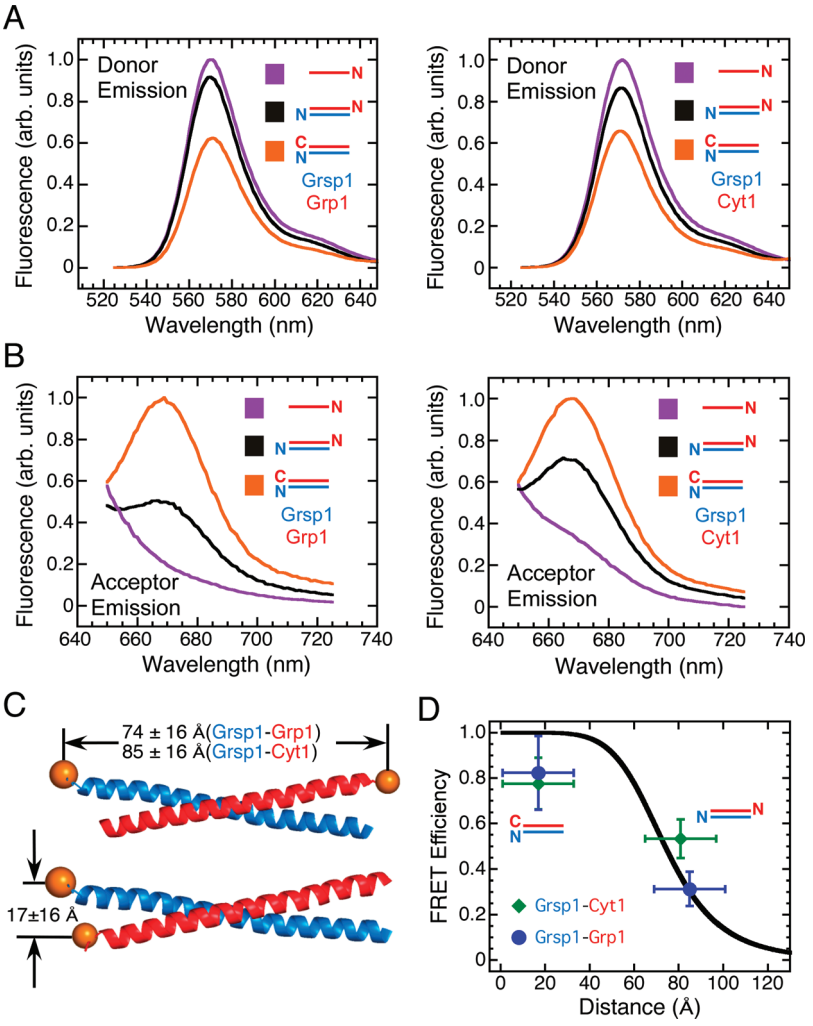

FIGURE 5: FRET analysis of Grsp1 complexes with Grp1 and Cytohesin-1. (A) Donor emission spectra for Grsp1−Grp1 and Grsp1−Cytohesin-1 complexes. The heptad repeat region of Cytohesin-1 (red lines) was labeled with Alexa-546 on a single cysteine at either the N- or C-terminus as indicated by N or C, respectively. The heptad repeat region of Grsp1 (light blue lines) was labeled with Alexa-647 on a single cysteine at the N-terminus. Samples were excited at 506 nm. (B) Sensitized emission spectra for Grsp1−Cytohesin-1 complexes labeled as in panel A. (C) Model coiled coil based on the crystal structure of EEA1. Measured distances correspond to the sulfur atoms in the cysteine residues to which the Alexa labels are attached. (D) Plot of the observed FRET efficiencies, corrected for labeling efficiency and concentration, vs the predicted distances from panel C.

homodimers. Note that Grp1, ARNO, and Cytohesin-1 constructs lacking the linker, PH domain, and C-terminal helix were used for the sedimentation equilibrium experiments with $Grsp1_{2-400}$ so that heterodimeric complexes could be distinguished from monomers and homodimers.

To determine the orientation of the Grsp1−Grp1 and Grsp1−Cytohesin-1 coiled coils, we conducted FRET experiments using Alexa Fluor-labeled peptides corresponding to the heptad repeat regions. For these experiments, the donor fluorophore (Alexa 546) was covalently attached to a single cysteine residue at the N- or C-terminus of Grp1 and Cytohesin-1 whereas the acceptor fluorophore (Alexa 647) was attached to a single cysteine residue at the N-terminus of Grsp1. As expected for an antiparallel orientation, the donor quenching as well as sensitized emission was considerably greater when the donor was attached to the C-terminus of the Grp1 or Cyothesin-1 heptad repeats (Figure 5A,B). To further analyze the FRET data, predicted donor−acceptor distances were estimated using the coiled-coil region in the crystal structure of the EEA1 C-terminus (*20*) as an approximate model (Figure 5C). On the basis of the estimated distances, the observed FRET efficiency was compared to the theoretical $1/R^6$ distance dependence calculated with a Forster radius R_0 of 74 Å for the Alexa-546−Alexa-647 donor−acceptor pair (Figure 5D). Taking into account the experimental error in the observed FRET efficiency (vertical bars) and the uncertainty in the estimated distances (horizontal bars), we conclude that the data are most consistent with either an antiparallel orientation or a mixed population with a predominately antiparallel orientation.

Recruitment of Grp1 to the plasma membrane in response to insulin stimulation requires binding of PtdIns(3,4,5)P_3 to the PH domain (*21*). In CHO-T cells, Grp1 and Grsp1 colocalize to membrane ruffles in response to insulin stimulation (*1*); however, it is unclear whether Grsp1 can partition with membranes in the absence of Grp1 or whether formation of the complex with Grsp1 affects membrane partitioning of Grp1. In addition, FERM domains in proteins such as ezrin and radixin have been shown to bind PtdIns(4,5)P_2 (*22*−*24*). Homology modeling suggests that the Grsp1 FERM domain conserves some of the basic residues implicated in the interaction with the PtdIns(4,5)P_2 headgroup in the crystal structure of the radixin FERM domain in complex with Ins(1,4,5)P_3 (*23*).

The ability of the Grsp1 FERM domain to bind Ins(1,4,5)P_3 or Ins(1,3,4,5)P_4 was assessed by isothermal titration microcalorimetry

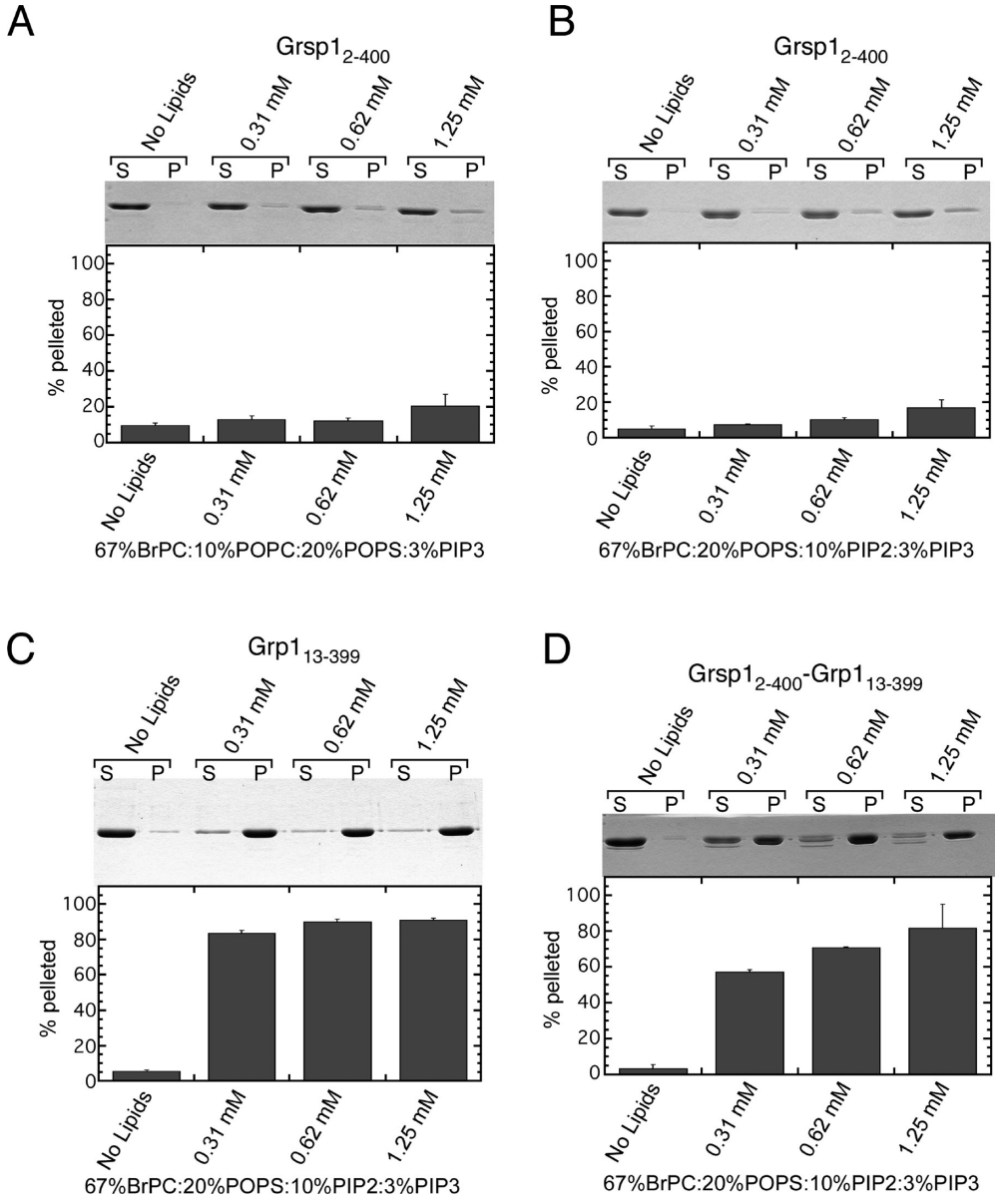

FIGURE 6: Sedimentation of Grsp1, Grp1, and the Grsp1−Grp1 complex with liposomes. The fraction pelleted was determined from the integrated band intensities corrected for background as described in Experimental Procedures. For the Grsp1−Grp1 complex, only the major band (higher-molecular mass species in panel D) was quantified. The lower-molecular mass species appears to be a truncated form of Grsp1 that does not bind Grp1. Bars and error bars represent the mean ± standard deviation for three experiments.

(ITC) at a protein concentration of 40 μM. Under the conditions used in these experiments, no detectable binding was observed (Figure S2 of the Supporting Information). Although it is hypothetically possible that binding occurs without a significant change in enthalpy and would therefore be difficult to detect by ITC, such entropically driven binding events are more typical of protein−protein interfaces that bury a substantial quantity of nonpolar surface area rather than the well-characterized high-affinity binding modes for polyphosphoinositides, which primarily involve ionic and/or polar interactions between basic residues and phosphate groups. To determine whether the oligomeric state or heterodimerization with Grsp1 directly influences headgroup binding, ITC was used to measure the affinity of Ins(1,3,4,5)P_4 for Grp1 homodimers or the Grp1 complex with Grsp1$_{2-400}$ (Figure S2 and Table S1 of the Supporting Information). In both cases, the dissociation constant (K_d) is similar to that of monomeric Grp1 constructs lacking the heptad repeat region (Table S1 of the Supporting Information) and is also similar to K_d values (27.3 and 32.2 nM) reported previously for the isolated PH domain (*6*, *25*).

The ITC experiments suggest that Grsp1$_{2-400}$ has weak if any affinity for the headgroups of PtdIns(4,5)P_2 and PtdIns(3,4,5)P_3; however, it is possible that a membrane environment may be required. For example, FYVE domains have weak affinity for the headgroup of PtdIns(3)P ($K_d \sim 30\ \mu$M) and even less affinity for soluble, short chain PtdIns(3)P analogues yet partition strongly with liposome membranes in a PtdIns(3)P-dependent manner. To address this possibility, we evaluated the partitioning of Grsp1$_{2-400}$, Grp1$_{13-399}$, and the Grp1$_{13-399}$−Grsp1$_{2-400}$ complex with phospholipid vesicles using a sedimentation assay. Whereas Grp1$_{13-399}$ partitions efficiently (~90% at 1.25 mM total phospholipid) with liposomes containing 20% PtdSer, 10% PtdIns(4,5)P_2, and 3% PtdIns(3,4,5)P_3, the majority of Grsp1$_{2-400}$ (~80−85% at a total phospholipid concentration of 1.25 mM) remains in the soluble fraction in both the presence and absence of PtdIns(4,5)P_2 (Figure 6 and Figure S3 of the

Supporting Information). The $Grsp1_{2-400}$−$Grp1_{13-399}$ complex also partitions efficiently (~80−90% at a total phospholipid concentration of 1.25 mM), although the fraction in the pellet appears to be somewhat reduced compared with that of Grp1 alone. Likewise, Grsp1 does not enhance partitioning of Grp1 with liposomes containing PtdIns(4,5)P_2 but not PtdIns(3,4,5)P_3.

DISCUSSION

The highly homologous proteins Grp1, ARNO, and Cytohesin-1 are 80−85% identical overall and >95% identical within the Sec7 and PH domains. Consistent with the high degree of sequence similarity, the proteins are effectively indistinguishable with respect to the exchange activity of the Sec7 domain and phosphoinositide recognition by the PH domain. Nevertheless, there is evidence of functional divergence. For example, a splice variant that differs only by the insertion of a single glycine residue in the $\beta1-\beta2$ loop of the PH domain has markedly reduced affinity for PtdIns(3,4,5)P_3 (*26*). In brain, Grp1 is predominately expressed as the high-affinity diglycine variant, whereas ARNO and Cytohesin-1 are predominately expressed as the low-affinity triglycine variant. In cells treated with the phorbal ester PMA, Cytohesin-1 and ARNO but not Grp1 are phosphorylated at PKC sites in the polybasic region (*27*, *28*). In addition to variations in alternative splicing and post-translation modification, sequence diversity within the heptad repeats (50−63% identical) may also contribute to functional differences. A classic example of this would be the bZIP family of transcription factors which utilize hetero and homo-oligomerization of a coiled-coil region to precisely modulate the transcriptional activity of target genes (*29*−*31*).

In this study, stable complexes of Grsp1 with Grp1 or Cytohesin-1 were isolated by gel filtration chromatography following incubation of stoichiometric amounts of the purified proteins. Conversely, only a fraction of ARNO (≤50%) was associated with Grsp1, and this fraction could not be increased by prolonged incubation. Although Grsp1 and Cytohesin-1 are monomeric under the conditions of these experiments, Grp1 and ARNO are uniformly homodimeric in the absence of Grsp1. Thus, whereas Grp1 homodimers readily re-equilibrate with Grsp1 to form more thermodynamically stable heterodimers, this is not the case for Grsp1−ARNO heterodimers, which are approximately as stable as ARNO homodimers. The substantially greater thermodynamic stability of Grsp1−Grp1 heterodimers compared with that of Grp1 homodimers provides a plausible thermodynamic explanation for the previously reported observation that Grsp1−Grp1 complexes could be detected by co-immunoprecipitation even though Grsp1−Grp1 homo-oligomers were not (*1*). The observed differences in the interaction of Grsp1 with ARNO might in principle reflect greater stability of the ARNO homodimer, lower stability of the Grsp1−ARNO heterodimer, or a combination of both. In any case, it is noteworthy that the extent of sequence divergence in the heptad repeat region is greater between Grp1 and ARNO (52% identical) than between Grp1 and Cytohesin-1 (63% identical). Most of the amino acid substitutions occur in the C-terminal half of the heptad repeat region and involve three of the hydrophobic residues in the predicted a and d positions, which are important for forming the helix interface between coiled coils (*29*, *32*). Finally, given that our studies employed a truncation construct of Grsp1 previously shown to be sufficient for Grp1 binding (but not tested with respect to ARNO or Cytohesin-1), it is possible that other regions of Grsp1 could contribute to the stability of complexes with ARNO or Cytohesin-1. However, the results of the co-immunoprecipitation experiments with the full-length proteins argue against this possibility.

Several proteins have been reported to associate with the heptad repeat regions of Grp1 family proteins, including Grsp1, CASP, and GRASP (*1*, *14*, *15*). In general, the stoichiometry and quaternary structure of these complexes have not been characterized. We have found that Grsp1 forms heterodimers with Grp1 and Cytohesin-1. The results of FRET experiments are consistent with an antiparallel coiled-coil arrangement or a mixture of species with a predominately antiparallel arrangement. This arrangement would in principle place the FERM domain of Grsp1 in the proximity of the Sec7 and PH domains of Grp1; however, formation of the Grsp1 complex does not appear to directly affect the functional properties of either domain.

FERM domains in some proteins have been shown to function as membrane targeting modules. In radixin, the headgroup of PtdIns(4,5)P_2 binds at the interface between two of the three subdomains that comprise the FERM domain (*33*, *34*). The headgroup binding site is located on an extended flat surface with a positive electrostatic potential that may contribute to membrane partitioning through nonspecific interactions with negatively charged phospholipids. Despite conservation of roughly 50% of the basic residues that contact the PtdIns(4,5)P_2 headgroup in the radixin FERM domain, the Grsp1 FERM domain shows no indication of binding to either Ins(1,4,5)P_3 or Ins(1,3,4,5)P_4 by ITC. Consistent with the absence of detectable headgroup binding, the partitioning of Grsp1 with liposomes is not enhanced by inclusion of 10% PtdIns(4,5)P_2 in the presence or absence of 3% PtdIns(3,4,5)P_3. Although a small fraction of Grsp1 was observed in the membrane fraction in both the presence and absence of PtdIns(4,5)P_2, indicative of a weak intrinsic ability to partition with acidic liposomes, Grsp1 did not appear to enhance the partitioning of 2G Grp1. However, it remains possible that Grsp1 could enhance partitioning with the 3G variants of Grp1 family proteins, which have considerably lower affinity for PtdIns(3,4,5)P_3 (*21*), or perhaps contribute to alternative targeting mechanisms described for Grp1 family proteins, including Arf6- and Arl4-dependent plasma membrane recruitment (*35*, *36*).

Finally, the FERM domains of ezrin, radixin, and moesin have been shown to bind polybasic regions in the cytoplasmic tails of integral membrane proteins (*13*). In contrast, we find no evidence of interaction of the Grsp1 FERM domain with the polybasic region of Grp1 (J. P. DiNitto, unpublished observations). Likewise, formation of the complex with Grsp1 does not affect the ability of the polybasic region to inhibit the exchange activity of the Sec7 domain (*16*). In view of these observations, it seems likely that the Grsp1 FERM domain will have functions that are yet to be identified, possibly including interactions with polybasic regions in proteins other than Grp1.

ACKNOWLEDGMENT

We thank Kim Crowley for assistance with analytical ultracentrifugation, Michael Czech for use of cell culture equipment, and Xiaochu Chen, Jes Klarlund, Tse-Chun Kuo, Xiarong Shi, and Qionglin Zhou for advice on co-immunoprecipitation experiments.

SUPPORTING INFORMATION AVAILABLE

Sedimentation equilibrium experiments for Grp1, ARNO, and Cytohesin-1 constructs lacking the heptad repeat region (Figure S1).

ITC analysis of Ins(1,3,4,5)P_4 and Ins(1,4,5)P_3 binding to Grp1, Grsp1, and the Grsp1−Grp1 complex (Figure S2), sedimentation of Grp1, Grsp1, and the Grsp1−Grp1 complex with liposomes (Figure S3), dissociation constants for inositol polyphosphate binding to Grp1, Grsp1, and the Grsp1−Grp1 complex (Table S1). This material is available free of charge via the Internet at http://pubs.acs.org.

REFERENCES

1. Klarlund, J. K., Holik, J., Chawla, A., Park, J. G., Buxton, J., and Czech, M. P. (2001) Signaling complexes of the FERM domain-containing protein GRSP1 bound to ARF exchange factor GRP1. *J. Biol. Chem. 276*, 40065–40070.
2. Langille, S. E., Patki, V., Klarlund, J. K., Buxton, J. M., Holik, J. J., Chawla, A., Corvera, S., and Czech, M. P. (1999) ADP-ribosylation factor 6 as a target of guanine nucleotide exchange factor GRP1. *J. Biol. Chem. 274*, 27099–27104.
3. Czech, M. P. (2000) PIP2 and PIP3: Complex roles at the cell surface. *Cell 100*, 603–606.
4. Katso, R., Okkenhaug, K., Ahmadi, K., White, S., Timms, J., and Waterfield, M. D. (2001) Cellular function of phosphoinositide 3-kinases: Implications for development, homeostasis, and cancer. *Annu. Rev. Cell Dev. Biol. 17*, 615–675.
5. Jackson, T. R., Kearns, B. G., and Theibert, A. B. (2000) Cytohesins and centaurins: Mediators of PI 3-kinase-regulated Arf signaling. *Trends Biochem. Sci. 25*, 489–495.
6. Kavran, J. M., Klein, D. E., Lee, A., Falasca, M., Isakoff, S. J., Skolnik, E. Y., and Lemmon, M. A. (1998) Specificity and promiscuity in phosphoinositide binding by pleckstrin homology domains. *J. Biol. Chem. 273*, 30497–30508.
7. Klarlund, J. K., Guilherme, A., Holik, J. J., Virbasius, J. V., Chawla, A., and Czech, M. P. (1997) Signaling by phosphoinositide-3,4,5-trisphosphate through proteins containing pleckstrin and Sec7 homology domains. *Science 275*, 1927–1930.
8. Kolanus, W. (2007) Guanine nucleotide exchange factors of the cytohesin family and their roles in signal transduction. *Immunol. Rev. 218*, 102–113.
9. Su, A. I., Wiltshire, T., Batalov, S., Lapp, H., Ching, K. A., Block, D., Zhang, J., Soden, R., Hayakawa, M., Kreiman, G., Cooke, M. P., Walker, J. R., and Hogenesch, J. B. (2004) A gene atlas of the mouse and human protein-encoding transcriptomes. *Proc. Natl. Acad. Sci. U.S.A. 101*, 6062–6067.
10. Wheeler, D. L., Church, D. M., Federhen, S., Lash, A. E., Madden, T. L., Pontius, J. U., Schuler, G. D., Schriml, L. M., Sequeira, E., Tatusova, T. A., and Wagner, L. (2003) Database resources of the National Center for Biotechnology. *Nucleic Acids Res. 31*, 28–33.
11. Watford, W. T., Li, D., Agnello, D., Durant, L., Yamaoka, K., Yao, Z. J., Ahn, H. J., Cheng, T. P., Hofmann, S. R., Cogliati, T., Chen, A., Hissong, B. D., Husa, M. R., Schwartzberg, P., O'Shea, J. J., and Gadina, M. (2006) Cytohesin binder and regulator (cybr) is not essential for T- and dendritic-cell activation and differentiation. *Mol. Cell. Biol. 26*, 6623–6632.
12. Lupas, A., Van Dyke, M., and Stock, J. (1991) Predicting coiled coils from protein sequences. *Science 252*, 1162–1164.
13. Yonemura, S., Hirao, M., Doi, Y., Takahashi, N., Kondo, T., and Tsukita, S. (1998) Ezrin/radixin/moesin (ERM) proteins bind to a positively charged amino acid cluster in the juxta-membrane cytoplasmic domain of CD44, CD43, and ICAM-2. *J. Cell Biol. 140*, 885–895.
14. Mansour, M., Lee, S. Y., and Pohajdak, B. (2002) The N-terminal coiled coil domain of the cytohesin/ARNO family of guanine nucleotide exchange factors interacts with the scaffolding protein CASP. *J. Biol. Chem. 277*, 32302–32309.
15. Nevrivy, D. J., Peterson, V. J., Avram, D., Ishmael, J. E., Hansen, S. G., Dowell, P., Hruby, D. E., Dawson, M. I., and Leid, M. (2000) Interaction of GRASP, a protein encoded by a novel retinoic acid-induced gene, with members of the cytohesin family of guanine nucleotide exchange factors. *J. Biol. Chem. 275*, 16827–16836.
16. DiNitto, J. P., Delprato, A., Gabe Lee, M. T., Cronin, T. C., Huang, S., Guilherme, A., Czech, M. P., and Lambright, D. G. (2007) Structural basis and mechanism of autoregulation in 3-phosphoinositide-dependent Grp1 family Arf GTPase exchange factors. *Mol. Cell 28*, 569–583.
17. Laue, T. M., Shah, B. D., Ridgeway, T. M., and Pelletier, S. L. (1992) Computer-aided interpretation of analytical sedimentation data for proteins. In Analytical Ultracentrifugation in Biochemistry and Polymer Science (Harding, S. E., Rowe, A. J., and Horton, J. C., Eds.) pp 90−125, Royal Society of Chemistry, Cambridge, U.K.
18. Chardin, P., Paris, S., Antonny, B., Robineau, S., Beraud-Dufour, S., Jackson, C. L., and Chabre, M. (1996) A human exchange factor for ARF contains Sec7- and pleckstrin-homology domains. *Nature 384*, 481–484.
19. Cherfils, J., Menetrey, J., Mathieu, M., Le Bras, G., Robineau, S., Beraud-Dufour, S., Antonny, B., and Chardin, P. (1998) Structure of the Sec7 domain of the Arf exchange factor ARNO. *Nature 392*, 101–105.
20. Dumas, J. J., Merithew, E., Sudharshan, E., Rajamani, D., Hayes, S., Lawe, D., Corvera, S., and Lambright, D. G. (2001) Multivalent endosome targeting by homodimeric EEA1. *Mol. Cell 8*, 947–958.
21. Klarlund, J. K., Tsiaras, W., Holik, J. J., Chawla, A., and Czech, M. P. (2000) Distinct polyphosphoinositide binding selectivities for pleckstrin homology domains of GRP1-like proteins based on diglycine versus triglycine motifs. *J. Biol. Chem. 275*, 32816–32821.
22. Niggli, V., Andreoli, C., Roy, C., and Mangeat, P. (1995) Identification of a phosphatidylinositol-4,5-bisphosphate-binding domain in the N-terminal region of ezrin. *FEBS Lett. 376*, 172–176.
23. Hamada, K., Shimizu, T., Matsui, T., Tsukita, S., and Hakoshima, T. (2000) Structural basis of the membrane-targeting and unmasking mechanisms of the radixin FERM domain. *EMBO J. 19*, 4449–4462.
24. Barret, C., Roy, C., Montcourrier, P., Mangeat, P., and Niggli, V. (2000) Mutagenesis of the phosphatidylinositol 4,5-bisphosphate (PIP(2)) binding site in the NH_2-terminal domain of ezrin correlates with its altered cellular distribution. *J. Cell Biol. 151*, 1067–1080.
25. Venkateswarlu, K., Gunn-Moore, F., Oatey, P. B., Tavare, J. M., and Cullen, P. J. (1998) Nerve growth factor- and epidermal growth factor-stimulated translocation of the ADP-ribosylation factor-exchange factor GRP1 to the plasma membrane of PC12 cells requires activation of phosphatidylinositol 3-kinase and the GRP1 pleckstrin homology domain. *Biochem. J. 335* (Part 1), 139–146.
26. Cronin, T. C., DiNitto, J. P., Czech, M. P., and Lambright, D. G. (2004) Structural determinants of phosphoinositide selectivity in splice variants of Grp1 family PH domains. *EMBO J. 23*, 3711–3720.
27. Dierks, H., Kolanus, J., and Kolanus, W. (2001) Actin cytoskeletal association of cytohesin-1 is regulated by specific phosphorylation of its carboxyl-terminal polybasic domain. *J. Biol. Chem. 276*, 37472–37481.
28. Frank, S. R., Hatfield, J. C., and Casanova, J. E. (1998) Remodeling of the actin cytoskeleton is coordinately regulated by protein kinase C and the ADP-ribosylation factor nucleotide exchange factor ARNO. *Mol. Biol. Cell 9*, 3133–3146.
29. O'Shea, E. K., Klemm, J. D., Kim, P. S., and Alber, T. (1991) X-ray structure of the GCN4 leucine zipper, a two-stranded, parallel coiled coil. *Science 254*, 539–544.
30. Burkhard, P., Stetefeld, J., and Strelkov, S. V. (2001) Coiled coils: A highly versatile protein folding motif. *Trends Cell Biol. 11*, 82–88.
31. Yamanaka, R., Lekstrom-Himes, J., Barlow, C., Wynshaw-Boris, A., and Xanthopoulos, K. G. (1998) CCAAT/enhancer binding proteins are critical components of the transcriptional regulation of hematopoiesis (Review). *Int. J. Mol. Med. 1*, 213–221.
32. O'Shea, E. K., Rutkowski, R., and Kim, P. S. (1989) Evidence that the leucine zipper is a coiled coil. *Science 243*, 538–542.
33. Lemmon, M. A. (2003) Phosphoinositide recognition domains. *Traffic 4*, 201–213.
34. Hamada, K., Shimizu, T., Yonemura, S., Tsukita, S., and Hakoshima, T. (2003) Structural basis of adhesion-molecule recognition by ERM proteins revealed by the crystal structure of the radixin-ICAM-2 complex. *EMBO J. 22*, 502–514.
35. Cohen, L. A., Honda, A., Varnai, P., Brown, F. D., Balla, T., and Donaldson, J. G. (2007) Active Arf6 recruits ARNO/cytohesin GEFs to the PM by binding their PH domains. *Mol. Biol. Cell 18*, 2244–2253.
36. Hofmann, I., Thompson, A., Sanderson, C. M., and Munro, S. (2007) The Arl4 family of small G proteins can recruit the cytohesin Arf6 exchange factors to the plasma membrane. *Curr. Biol. 17*, 711–716.